doi:10.1017/S1431927614002220
Microsc. Microanal. 20 (Suppl 3), 2014

Absorption Corrections for a Four-Quadrant SuperX EDS Detector

F. Yang[1], F. Scheltens[1], D. McComb[1], D.B. Williams[1], and M. De Graef[2]

[1.] Dept. of Materials Science and Engineering, Ohio State Univ., Columbus OH 43210, USA
[2.] Dept. of Materials Science and Engineering, Carnegie Mellon Univ., Pittsburgh PA 15213, USA

Consider a four-quadrant detector consisting of four circular active regions of area A_q each, placed symmetrically around the sample, as shown schematically in Fig. 1(a). The sample holder is inserted from the right, and the quadrants are 90° apart, oriented symmetrically at ±45° with respect to the primary tilt axis. The specimen tilt angles are labeled α and β, with positive angles corresponding to counterclockwise rotations. Each detector quadrant is located above the plane of the specimen and is tilted from the vertical plane by an angle δ_d; the angle between the line connecting the center of a quadrant D with the eucentric point S and the horizontal plane is labeled α_d (Fig. 1(b)). The active circular regions have a radius of R_d, and a distance to the eucentric point of r_d; the detector opening angle is $R = R_d/r_d$. When $\bar{R}$ is not negligible, as is the case for a SuperX detector, then the x-ray photon path length inside the sample becomes a function of the position on the detector where the pho-ton hits; the absorption correction factor must thus involve an integration over the detector surface area.

The path length τ inside the sample for an x-ray photon leaving P_0 and traveling towards the point P_1 on the detector can be expressed as a fraction s of the distance between P_0 and P_l:

$$\tau(x_d, z_d) = s(x_d, z_d)\sqrt{x_d^2 + z_d^2 + r_d^2} \quad \text{with} \quad s(x_d, z_d) = -\frac{\mathbf{n}\cdot\mathbf{P}_0}{\mathbf{n}\cdot(\mathbf{P}_1 - \mathbf{P}_0)},$$

where $(x_d,\ z_d)$ are the in-plane detector coordinates of the point P_0. Using the quadrant numbering of Fig. 1(a), one can show that the thickness-integrated dimensionless absorption correction factor for quadrant i is given by:

$$C_i(\mu t) = \left[\frac{1}{\pi\bar{R}^2}\iint_D \mathrm{d}\bar{x}\mathrm{d}\bar{z}\,\frac{1 - e^{-\mu t f_i(\bar{x},\bar{z})}}{\mu t f_i(\bar{x},\bar{z})}\right]^{-1},$$

where

$$f_i(\bar{x},\bar{z}) = \frac{\sqrt{\bar{x}^2 + \bar{z}^2 + 1}}{a_i\bar{x} + b_i\bar{z} + c_i}$$

with

$$\begin{cases} a_i = s_i \sin\alpha\cos\beta + c_i \sin\beta; \\ b_i = \cos\delta_d \cos\alpha\cos\beta + \sin\delta_d(c_i \sin\alpha\cos\beta - s_i\sin\beta); \\ c_i = \sin\alpha_d\cos\alpha\cos\beta - \cos\alpha_d(c_i\sin\alpha\cos\beta - s_i\sin\beta), \end{cases}$$

and $\bar{x} = x/r_d$ and $\bar{z} = y/r_d$. This integral poses no numerical difficulties, as the integrand is well behaved, even when the denominator of f_i vanishes (in which case the integrand equals unity). In the absence of sample tilt ($\alpha = \beta = 0$), the expression for f_i reduces to

$$f_i(\bar{x},\bar{z}) = \frac{z\sqrt{\bar{x}^2 + \bar{z}^2 + 1}}{\cos\delta_d\bar{z} + \sin\alpha_d},$$

which, in the limit of vanishing detector radius R_d, becomes

$$f_i = \frac{z}{\sin\alpha_d} = z\csc\alpha_d,$$

i.e., the standard result for a small distant detector. Since the four quadrant detectors are located symmetrically with respect to the specimen we have the following symmetry relations between the correction factors:

$$C_2(\alpha,\beta;\mu t) = C_1(\alpha,-\beta;\mu t), \quad C_3(\alpha,\beta;\mu t) = C_1(-\alpha,-\beta;\mu t), \quad C_4(\alpha,\beta;\mu t) = C_1(-\alpha,\beta;\mu t),$$

so that we only need to compute $\boldsymbol{C_1}(\alpha,\ \beta;\ \mu t)$ over the entire range of tilt angles. Fig. 2 shows a contour plot of the inverse correction factor $1/C_1(\alpha,\ \beta;\ \mu t)$ as a function of tilt angles $(\alpha,\ \beta)$ and for the detector parameters indicated in the upper left corner.

References

[1] MDG was supported by the Air Force Office of Scientific Research, MURI contract #
FA9550-12-1-0458.

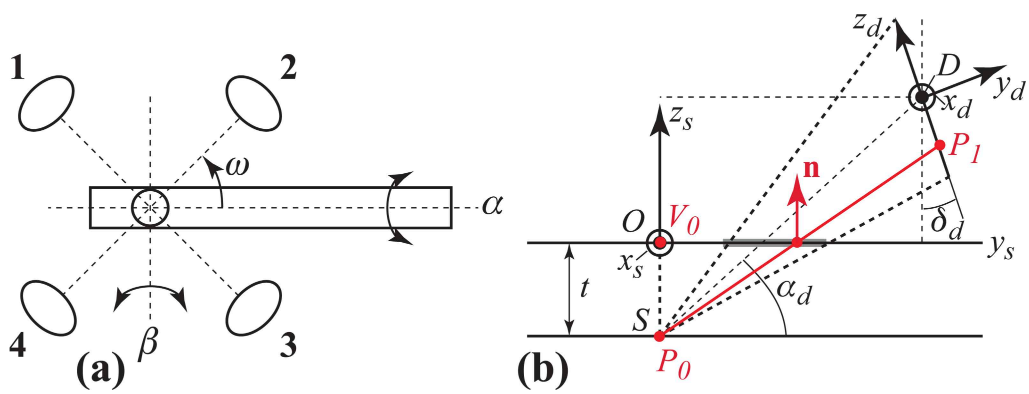

Figure 1. (a) Schematic representation of a double tilt sample holder and four quadrant detectors placed symmetrically around the specimen; (b) Schematic of the specimen with thickness t, and a single circular quadrant detector

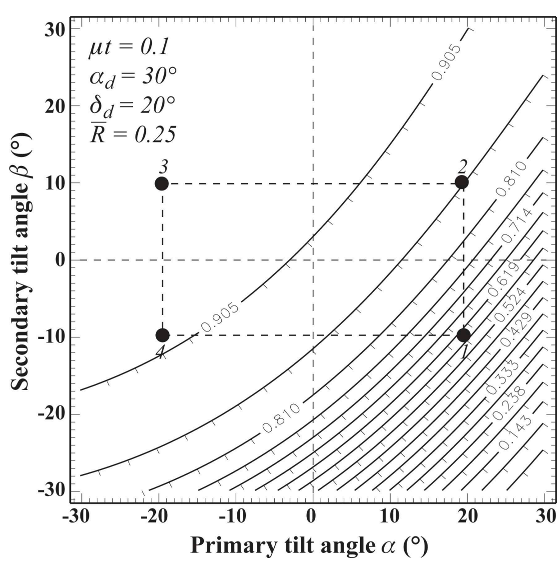

Figure 2. Contour plot of $1/C_1$ $(\alpha,\ \beta;\ \mu t)$ for the detector parameters indicated in the upper left corner. The rectangle superimposed on the plot shows the symmetry relations between an arbitrary pair of angles $(\alpha,\ \beta)$ and the corresponding points for the other three detector quadrants.

https://doi.org/10.1017/S1431927614002220 Published online by Cambridge University Press